X. STATISTICAL COMMUNICATION THEORY

Prof. Y. W. Lee
A. G. Bose
J. Y. Hayase
S. G. Margolis
C. E. McGinnis
S. D. Pezaris
W. B. Smith
R. E. Wernikoff

A. A THEOREM CONCERNING NOISE FIGURES

An expression is obtained for the greatest lower bound of the noise figure of a system consisting of n identical tubes whose plate signals are directly added and whose inputs are obtained through a linear passive coupling network from a source having an internal impedance R_s. It is found that the optimum attainable noise figure of such a system is equal to the optimum noise figure of a circuit consisting of one such tube and an appropriate coupling network.

Introduction

The electron tube, while providing amplification, is a source of noise. Thus, for the detection of weak signals it is advantageous to design the circuitry associated with the amplifier to maximize the signal-to-noise ratio at the output of the amplifier when it is fed from a given source. That is, it is advantageous to minimize the noise figure of the circuit. In the past, attempts have been made to obtain smaller noise figures than obtainable with one tube by using circuits involving more tubes; the plate signal of each tube was added directly to the plate signals of the other tubes to form the output of the circuit. Such attempts have been motivated by the hope that smaller noise figures could be obtained by taking advantage of the incoherency of noise voltages from different noise sources. (The signal at the output of each tube adds coherently while the noise arising from different tubes adds incoherently.) It is the purpose of this work to prove that the noise figure of a circuit involving n identical tubes, connected as indicated above, is at best equal to the optimum noise figure attainable with the use of only one tube and an appropriate coupling network.

Proof

The noise figure calculations are based on a unit bandwidth centered about a frequency f. It is assumed that each tube may be represented, as far as noise figure calculations are concerned, by a shunt resistance R_g and a series equivalent resistance R_{eq} followed by an ideal noiseless tube. According to this assumption, the equivalent circuit is shown in Fig. X-1. Associated with each resistance is a series thermal noise voltage source. For a resistance R the open circuit mean square voltage per unit bandwidth is $4KT\rho R$, where: K = Boltzmann's constant;

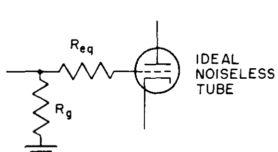

Fig. X-1
Noise equivalent circuit of conventional amplifier tube.

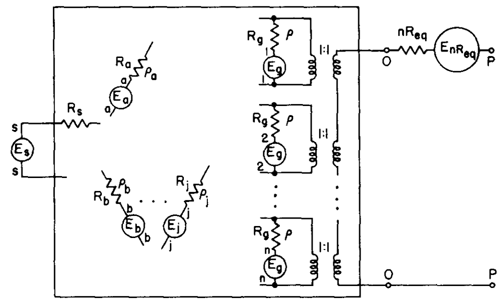

Fig. X-2

Equivalent circuit (for noise figure calculation) of a source coupled through a general coupling network to n tubes whose plate signals are directly added.

T = temperature in degrees Kelvin; ρ = a positive factor used to take into account the equivalent noise temperature of the resistance. We shall call it the equivalent temperature factor.

An equivalent circuit (as far as noise figure calculations are concerned) of a system consisting of n identical tubes whose plate signals are added directly and whose grid signals are obtained through a general linear passive coupling network from a source with impedance R_s is shown in Fig. X-2. The ideal noiseless tubes of Fig. X-1 have been replaced by ideal transformers whose turns ratios have conveniently been chosen to be unity. There is no loss of generality in this choice since a change in the output level affects both signal and noise and thus leaves the signal-to-noise ratio unaltered. The circuit shown in Fig. X-2, with the terminals p-p open circuited, has the same noise figure as the system of n tubes under consideration. The resistances R_a through R_j represent all the resistors in the coupling network. The sources in series with each resistor are the equivalent noise voltage sources. The equivalent temperature factor of each R_g is ρ. The equivalent temperature factor of each of the resistors in the coupling network is arbitrary and is denoted in Fig. X-2 by the symbol ρ with a subscript corresponding to the resistor with which it is associated.

For a linear system, the ratio of the open circuit voltage response at terminals k-k to a voltage excitation at terminals j-j can be expressed in terms of the short circuit admittance parameters as:

$$G(\omega) = -\frac{y_{kj}}{y_{kk}} \tag{1}$$

The noise figure of a system is defined as

$$F = 1 + \frac{\text{"noise power" at the output caused by noise sources in the system}}{\text{"noise power" at the output caused by noise generated in the source impedance}} \tag{2}$$

The term "noise power" denotes the integral of the power spectrum of the open circuit voltage over a unit bandwidth centered about a frequency f. Making use of Eqs. 1 and 2, the noise figure for the system shown in Fig. X-2 can be written as

$$F = 1 + \frac{n\,R_{eq} + \dfrac{\rho\,R_g}{|y_{oo}|^2}\left(|y_{01}|^2 + |y_{02}|^2 + \ldots + |y_{on}|^2\right) + \dfrac{1}{|y_{oo}|^2}\left(\rho_a R_a\,|y_{oa}|^2 + \ldots + \rho_j R_j\,|y_{oj}|^2\right)}{R_s\,\dfrac{|y_{os}|^2}{|y_{oo}|^2}} \tag{3}$$

Certainly the right-hand side of this equation will not increase if we assume, for the purpose of calculation, that each of the resistors R_a through R_j in the coupling network has an equivalent temperature factor equal to zero. Equation 3 then becomes

$$F \geq 1 + \frac{n\,R_{eq}|y_{oo}|^2 + \rho\,R_g\left(|y_{01}|^2 + |y_{02}|^2 + \ldots + |y_{on}|^2\right)}{R_s\,|y_{os}|^2} \tag{4}$$

Notice that the equality sign holds in Eq. 4 if R_a through R_j in Eq. 3 are zero.

Let g_{oo} be the real part of the output admittance y_{oo}. As a consequence of the relation $|y_{oo}| \geq g_{oo}$ we can write

$$F \geq 1 + \frac{n\,R_{eq}\,g_{oo}^2 + \rho\,R_g\left(|y_{01}|^2 + |y_{02}|^2 + \ldots + |y_{on}|^2\right)}{R_s\,|y_{os}|^2} \tag{5}$$

Notice that the equality sign in Eq. 5 holds when the condition stated under Eq. 4 holds and, at the same time, the output admittance is real.

In order to reduce the number of variables in this expression for F (Eq. 5) let us make use of power relations at the output terminals 0-0. Let P be the power absorbed by the system when one volt is applied at the output terminals and all other voltage sources are shorted.

Then

$$P = R_s|y_{so}|^2 + R_g\left(|y_{10}|^2 + |y_{20}|^2 + \ldots + |y_{no}|^2\right) + P_1 \tag{6}$$

where P_1 is the power absorbed in the coupling circuit resistors R_a through R_j and is therefore equal to or greater than zero. Furthermore, for the particular excitation mentioned above, P is just equal to g_{oo}. Using this fact and the relation $y_{ik} = y_{ki}$ for a bilateral network we obtain the equation

$$g_{oo} = R_s |y_{os}|^2 + R_g \left(|y_{01}|^2 + |y_{02}|^2 + \ldots + |y_{on}|^2\right) + P_1 \tag{7}$$

Using Eq. 7 in Eq. 5 we have

$$F \geqslant 1 - \rho + \frac{n R_{eq} g_{oo}^2 + \rho g_{oo} - \rho P_1}{R_s |y_{so}|^2} \tag{8}$$

In order to simplify this expression further let us again consider the system shown in Fig. X-2. We shall excite the system at the terminals 0-0 with a unit voltage source. For convenience Fig. X-2 is redrawn in Fig. X-3 with the resistances R_g referred to the secondary of the ideal one-to-one ratio transformers. We desire to find a relation between g_{oo} and $|y_{os}|$. In obtaining this relation it is convenient to make use of the following inequality (the proof of this inequality is given in the following subsection):

$$\sum_{k=1}^{n} |e_k|^2 \geqslant \frac{1}{n} \left| \sum_{k=1}^{n} e_k \right|^2 \tag{9}$$

For a one-volt excitation at terminals 0-0 it is seen, from power considerations and the use of Eq. 7, that

$$\begin{aligned} g_{oo} &= \frac{1}{R_g}\left(|e_1|^2 + |e_2|^2 + \ldots + |e_n|^2\right) + R_s |y_{so}|^2 + P_1 \\ &\geqslant R_s |y_{so}|^2 + \frac{1}{n R_g} + P_1 \end{aligned} \tag{10}$$

Notice that the equality sign holds if the coupling network is symmetrical with respect to its n outputs. Substitution of the expression for $|y_{so}|^2$, obtained from Eq. 10, in Eq. 8 yields

$$F \geqslant 1 - \rho + \frac{n R_{eq} g_{oo}^2 + \rho g_{oo} - \rho P_1}{g_{oo} - \frac{1}{n R_g} - P_1} = A \tag{11}$$

The quantity A is thus expressed as an explicit function of the two variables g_{oo} and P_1. We desire to minimize A with respect to these two variables. It can be seen from

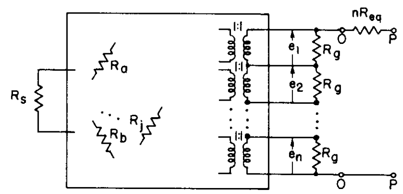

Fig. X-3

Redrawn with all the noise voltage sources set to zero and with the resistances R_g referred to the secondary of the ideal transformers.

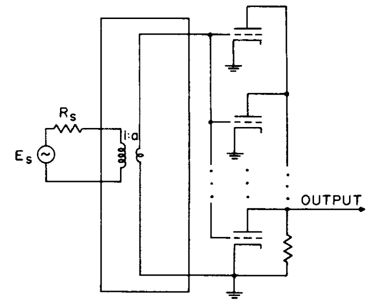

Fig. X-4

Example of a circuit using n tubes and having the minimum obtainable noise figure of one tube.

Eq. 7 that g_{oo} and P_1 are, in general, dependent quantities. If A is minimized with respect to g_{oo} and P_1, considered as independent variables, the minimum value thus obtained will certainly be equal to, or less than, the minimum obtained when the constraints are imposed. Further, it will be seen that in this particular case the minimums are equal since a coupling network corresponding to the minimum A will be physically realizable.

Proceeding with the minimization, Eq. 11 yields

$$\frac{\partial A}{\partial P_1} = \frac{\dfrac{\rho}{n R_g} + n R_{eq} g_{oo}^2}{\left(g_{oo} - \dfrac{1}{n R_g} - P_1\right)^2} > 0 \tag{12}$$

A justification of the inequality symbol in this equation is necessary. Referring to Eq. 10 we see that the denominator in Eq. 12 is always positive and greater than zero. (It can be zero only for the trivial case in which $R_s |y_{so}|^2$ is zero, a case which clearly is of no interest since it implies either a zero impedance source or no transmission from input to output, that is, $y_{so} = 0$.) Since ρ is a positive quantity, it is clear that the numerator of Eq. 12 is greater than zero and that the inequality symbol is valid as shown.

Since $(\partial A/\partial P_1) > 0$ and since $P_1 \geqslant 0$, the minimum value of A occurs for $P_1 = 0$. We next find the optimum g_{oo} which gives the minimum A for $P_1 = 0$.

$$A_{(P_1=0)} = 1 - \rho + \frac{n R_{eq} g_{oo} + \rho}{1 - \dfrac{1}{n R_g g_{oo}}} \tag{13}$$

$$\frac{\partial A_{(P_1=0)}}{\partial g_{oo}} = \frac{n R_{eq} - \dfrac{2 R_{eq}}{R_g g_{oo}} - \dfrac{\rho}{n R_g g_{oo}^2}}{\left(1 - \dfrac{1}{n R_g g_{oo}}\right)^2} = 0 \tag{14}$$

For the same reasons discussed earlier relative to Eq. 12, the denominator of Eq. 14 is always greater than zero. Thus by setting the numerator equal to zero we obtain the optimum value of g_{oo}.

$$g_{oo_{opt}} = \frac{1}{n R_g} \left[1 + \left(1 + \frac{\rho R_g}{R_{eq}}\right)^{1/2}\right] \tag{15}$$

Substituting this optimum value of g_{oo} into Eq. 13 we obtain the minimum value of A.

$$A_{min} = 1 + 2 \frac{R_{eq}}{R_g} \left[1 + \left(1 + \frac{\rho R_g}{R_{eq}}\right)^{1/2}\right] \tag{16}$$

The fact that the value of A obtained by this procedure is a minimum can be verified by considering Eqs. 10 and 13.

In view of Eqs. 11 and 15 we can write

$$F \geqslant 1 + 2 \frac{R_{eq}}{R_g} \left[1 + \left(1 + \frac{\rho R_g}{R_{eq}}\right)^{1/2}\right] \tag{17}$$

The fact that the equality sign in this inequality is valid is most readily demonstrated by presenting an example in which it holds. The construction of an example is facilitated by noting the sufficient conditions for the validity of the equality sign in the relations of Eqs. 4, 5, and 10. These conditions are stated immediately following their respective equations. Such an example is shown in Fig. X-4. All of the n tubes are in parallel, and the general coupling network is just an ideal transformer with an appropriate turns ratio. A straightforward calculation shows that this circuit has the noise figure given by Eq. 17 with the equality sign when each tube has the input resistance R_g (with an equivalent temperature factor ρ) and the equivalent shot noise resistance R_{eq}.

The interesting result is that the right-hand member of Eq. 17 is independent of n and is exactly the optimum noise figure attainable using a single tube. For $R_{eq}/R_g \ll 1$, Eq. 17 reduces to the more familiar form for the noise figure of a single stage (1):

$$F \geq 1 + 2\left(\frac{\rho\, R_{eq}}{R_g}\right)^{1/2} \tag{18}$$

Derivation of Inequality 9

Derivation of the inequality:

$$\sum_{k=1}^{n} |e_k|^2 \geq \frac{1}{n}\left|\sum_{k=1}^{n} e_k\right|^2 \tag{9}$$

Since the magnitude of the sum of complex numbers is less than or equal to the sum of the magnitudes we can write

$$\frac{1}{n}\left|\sum_{k=1}^{n} e_k\right|^2 \leq \frac{1}{n}\left(\sum_{k=1}^{n} |e_k|\right)^2 \tag{19}$$

But

$$\frac{1}{n}\left(\sum_{k=1}^{n} |e_k|\right)^2 = \sum_{k=1}^{n} |e_k|^2 - \frac{1}{n}\left\{(n-1)\sum_{k=1}^{n} |e_k|^2 - \sum_{\substack{i,k \\ i\neq k}} |e_i e_k|\right\}$$

$$= \sum_{k=1}^{n} |e_k|^2 - \frac{1}{2n}\sum_{\substack{i,k \\ i\neq k}} \left(|e_i| - |e_k|\right)^2 \leq \sum_{k=1}^{n} |e_k|^2 \tag{20}$$

Thus, combining Eq. 19 and Eq. 20 we have the desired result:

$$\sum_{k=1}^{n} |e_k|^2 \geq \frac{1}{n}\left|\sum_{k=1}^{n} e_k\right|^2$$

A. G. Bose, S. D. Pezaris

References

1. G. E. Valley, Jr. and H. Wallman, M.I.T. Radiation Laboratory Series, Vol. 18 (McGraw-Hill Book Company, Inc., New York, 1948) p. 640.

B. THE WIENER THEORY OF NONLINEAR SYSTEMS

Introduction

Briefly stated, the objectives of Dr. Wiener's method are to characterize nonlinear systems independent of their input and to present a method for synthesizing the systems from their characterizing parameters. An operator relating the input and output of the nonlinear system is defined in such a way that the parameters which characterize the system can be evaluated experimentally.

The method is confined to those nonlinear systems in which the remote past becomes less and less relevant to the behavior of the system as we push it back in time. It is further restricted to those systems in which fast changes in the output, relative to the input, do not occur. The reason for these restrictions, as will become apparent, is to avoid an excessive number of terms in the Laguerre and Hermite expansions respectively.

As Dr. Wiener has shown, the proper probe for the general investigation of nonlinear systems is the output of a shot-effect generator (gaussian noise with a flat power spectrum). The shot effect is the most general probe and enables nonlinear systems to be classified for all inputs (1).

Definitions

To simplify the description of the method, it is convenient at this point to define certain quantities and relations that are useful in the development of the method.

A. The nth Laguerre polynomial,

$$L_n(x) = \frac{1}{n!} e^x \frac{d^n}{dx^n} (x^n e^{-x})$$

B. The normalized Laguerre functions $h_n(x)$ are defined

$$h_n(x) = e^{-x/2} L_n(x) \tag{1}$$

The following orthogonality relation exists for these functions:

$$\int_0^\infty h_m(x)\, h_n(x)\, dx = \begin{cases} 1 \text{ if } m = n \\ 0 \text{ if } m \neq n \end{cases} \tag{2}$$

C. The nth Hermite polynomial

$$H_n(x) = (-1)^n e^{x^2} \left(\frac{d}{dx}\right)^n e^{-x^2}$$

D. The normalized Hermite polynomials $\phi_n(x)$ are defined

$$\phi_n(x) = \frac{H_n(x)}{\left(2^n\ n!\ (\pi)^{1/2}\right)^{1/2}} \tag{3}$$

E. The normalized Hermite functions are defined

$$\psi_n(x) = e^{-x^2/2}\ \phi_n(x) \tag{4}$$

These functions form a normal orthogonal set over the interval $-\infty$ to ∞. Consequently, we have the relation

$$\int_{-\infty}^{\infty} \phi_m(x)\ \phi_n(x)\ e^{-x^2}\ dx = \begin{cases} 1 & m = n \\ 0 & m \neq n \end{cases} \tag{5}$$

Description of the General Method of Characterization and Synthesis

Now let us consider a nonlinear system whose input and output are the stationary time series x(t) and y(t), respectively. In general, y(t) is some function of the past of x(t). Consequently, it is of interest to obtain a set of parameters which characterize the past of x(t). The past of x(t) can be expanded in a series of Laguerre functions as indicated in Eq. 6

$$x(-t) = \sum_n u_n\ h_n(t) \tag{6}$$

The Laguerre functions form a complete set over the interval zero to infinity and the coefficients u_n form a set of variables which characterize the past of x(t).

These Laguerre coefficients of the past of a time function x(t) are easily generated in practice. They are simply the output of a Laguerre network (a network whose impulse response is $h_n(t)$) whose input is x(t). This can be seen as follows. Referring to Fig. X-5, the output at the present time (t=0) is given by the convolution of x(t) with $h_n(t)$. That is,

$$y(0) = \int_{-\infty}^{0} x(z)\ h_n(0-z)\ dz = \int_{0}^{\infty} x(-z)\ h_n(z)\ dz \tag{7}$$

Let us compare this expression for $y_n(0)$ with the expression for u_n which is obtained

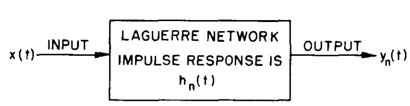

Fig. X-5
Block diagram of Laguerre network.

from Eq. 6 by making use of the orthogonality property of Eq. 2. The latter expression is

$$u_n = \int_0^\infty x(-t)\, h_n(t)\, dt \tag{8}$$

Comparison of Eqs. 7 and 8 shows that $y_n(0) = u_n$. Thus we have demonstrated that the coefficients u_n can be generated by the method shown in Fig. X-5. The actual form of the Laguerre network and the method of synthesis of this network will not be discussed here. For a complete discussion of these topics the reader is referred to reference 2.

Since the set of coefficients u_n characterize the past of x(t), any quantity dependent only on the past of x(t) may be represented as a function of these coefficients. Thus for the nonlinear system with input x(t) and output y(t) we can write

$$y(t) = F\left[u_1, u_2, \ldots, u_s\right] \tag{9}$$

For reasons that will soon become apparent it is convenient to express this function F as a Hermite function expansion of the variables u_1 through u_s. We then have

$$y(t) = \sum_i \sum_j \cdots \sum_h a_{i,j,\ldots,h}\, \phi_i(u_1)\, \phi_j(u_2) \ldots \phi_h(u_s)\, e^{-\frac{u_1^2+u_2^2+\ldots+u_s^2}{2}} \tag{10}$$

In order to simplify this equation let $\Phi(\alpha)$ represent the polynomial $\phi_i(u_1)\ldots\phi_h(u_s)$, and A_α represent the corresponding value of $a_{i,j,\ldots,h}$. Then Eq. 10 becomes

$$y(t) = \sum_\alpha A_\alpha\, \Phi(\alpha)\, e^{-\frac{u_1^2+\ldots+u_s^2}{2}} \tag{11}$$

If, in Eq. 10, the indices $i, j, \ldots, h$ range from 0 to $N - 1$, then α ranges from 0 to $N^s - 1$.

To characterize the nonlinear system, it is necessary to evaluate the coefficients A_α in Eq. 11. To this end, consider the time average

$$\overline{y(t)\, \Phi(\beta)} = \overline{\sum_\alpha A_\alpha\, \Phi(\alpha)\, \Phi(\beta)\, e^{-\frac{u_1^2+\ldots+u_s^2}{2}}} \tag{12}$$

Let us take advantage of the ergodic theorem in evaluating the right-hand member of this equation. We then have

$$\overline{y(t)\ \Phi(\beta)} = \sum_{\alpha} A_{\alpha} \int_{-\infty}^{\infty} \cdots \int_{-\infty}^{\infty} \Phi(\alpha)\ \Phi(\beta)\ e^{-\frac{u_1^2 + \ldots + u_s^2}{2}}\ P(u_1, \ldots, u_s)\ du_1 \ldots du_s \tag{13}$$

As mentioned earlier, the probe for the investigation of the nonlinear system is the output of a shot-effect generator. Thus, for the evaluation of the coefficients A_{α} in Eq. 13, the input x(t) to the nonlinear system is a gaussian signal with a flat power spectrum. Now recall that the parameters u_1 through u_s which characterize the past of x(t) can be obtained as the outputs of the linear passive Laguerre network whose input is x(t). Thus, if x(t) has a gaussian distribution, then u_1 through u_s all have gaussian distributions. In fact, it can be shown from the properties of the Laguerre network, or from the definition of the Laguerre functions, that u_1 through u_s all have independent normalized gaussian distributions when x(t) is gaussian with a flat power spectrum and the proper variance. Thus we have

$$P(u_1, \ldots, u_s) = (2\pi)^{-s/2}\ e^{-\frac{u_1^2 + \ldots + u_s^2}{2}} \tag{14}$$

so that Eq. 13 becomes

$$\overline{y(t)\ \Phi(\beta)} = (2\pi)^{-s/2} \sum_{\alpha} A_{\alpha} \int_{-\infty}^{\infty} \cdots \int_{-\infty}^{\infty} \Phi(\alpha)\ \Phi(\beta)\ e^{-(u_1^2 + \ldots + u_s^2)}\ du_1 \ldots du_s \tag{15}$$

The reason for the choice of Hermite functions for the expansion of Eq. 9 now becomes apparent. The joint gaussian probability density (Eq. 14) supplies the necessary exponential factor in the Hermite function expansion (Eq. 12) to enable us to take advantage of the orthogonality relation of Eq. 5 in evaluating the coefficients A_{α}. Taking advantage of this orthogonality we have:

$$A_{\beta} = (2\pi)^{s/2}\ \overline{y(t)\ \Phi(\beta)} \tag{16}$$

The A_{α}'s, together with a knowledge of the number of Laguerre coefficients used, serve to characterize the nonlinear system under test. The setup for the experimental evaluation of the coefficients A_{α} is shown in Fig. X-6.

Now let us consider the problem inverse to that discussed above. Suppose we are given a set of coefficients A_{α} and asked to find a nonlinear system corresponding to these coefficients. Equation 11 is the guide for the synthesis problem. This equation tells us that, for each α, we must form $\Phi(\alpha)$ and multiply it by A_{α} and the exponential

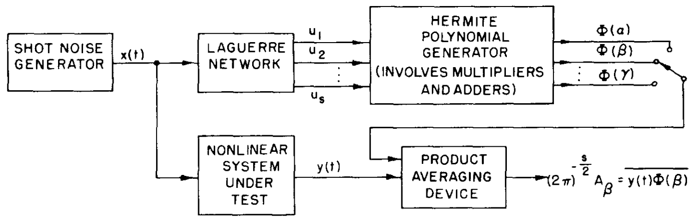

Fig. X-6

Block diagram of the circuitry for the classification of nonlinear systems.

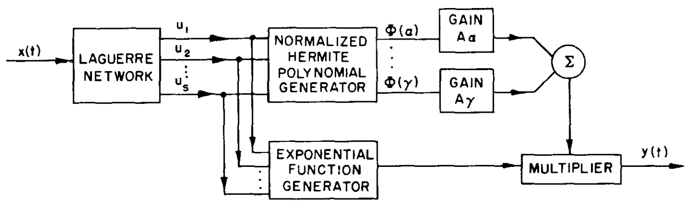

Fig. X-7

Block diagram for the synthesis of nonlinear systems.

$\exp -\left(u_1^2 + \ldots + u_s^2\right)/2$. Then each such product must be added. In practice, the number of multipliers is reduced if we first form the sum of the products $A_\alpha\ \Phi(\alpha)$ and then multiply by the exponential function.

The exponential function, $\exp -\left(u_1^2 + \ldots + u_s^2\right)/2$, can be obtained as the product of s exponential function generators whose inputs are respectively u_1 through u_s. Such generators give an output of $\exp -(x^2/2)$ when the input is x. They are realizable, among other ways, in the form of a small cathode-ray tube with a special target to generate the $\exp -(x^2/2)$ function.

The block diagram of the circuitry used for the synthesis procedure is shown in Fig. X-7.

Example

In order to fix ideas, let us consider a simple example which is particularly suited to characterization and synthesis by Dr. Wiener's method. Let the given nonlinear system contain no storage elements. Further let its input-output characteristic be given by the equation

$$y(t) = e^{-x^2(t)/2} \tag{17}$$

where x(t) is the input and y(t) is the output.

In both the characterization and synthesis procedures described, the Laguerre network is used to introduce dependence of the output upon the past of the input. The nonlinearity is brought about by the Hermite polynomial generator. For the simple example under consideration, there is no dependence upon the past and thus we can by-pass the Laguerre network. In the experimental procedure, the fact that this nonlinear system has no storage can easily be determined from the results of a priori tests made on the system.

To proceed with the characterization of the simple example, we notice that as a result of by-passing the Laguerre network (Fig. X-6) the variables u_1 through u_s are replaced by the single variable x(t). Equation 10 then becomes:

$$y(t) = \sum_i a_i \phi_i(x) e^{-x^2/2} \tag{18}$$

Equation 16 becomes

$$a_i = (2\pi)^{1/2} \overline{y(t) \phi_i(x)} \tag{19}$$

Let us make use of the ergodic theorem to evaluate this time average as an ensemble average. Using Eq. 17 we can write

$$a_i = (2\pi)^{1/2} \int_{-\infty}^{\infty} \phi_i(x) e^{-x^2/2} p(x) dx \tag{20}$$

But since, in the test setup, x(t) is the output of an ideal shot-effect generator, the probability density of x is

$$p(x) = \frac{1}{(2\pi)^{1/2}} e^{-x^2/2} \tag{21}$$

Thus

$$a_i = \int_{-\infty}^{\infty} \phi_i(x) e^{-x^2} dx \tag{22}$$

Referring to Eq. 3 and the definition of the Hermite polynomial, it is seen that

$$\phi_o(x) = \pi^{-1/4} \tag{23}$$

With this result, Eq. 22 becomes

$$a_i = \pi^{1/4} \int_{-\infty}^{\infty} \phi_i(x) \phi_o(x) e^{-x^2} dx \tag{24}$$

As a consequence of the orthogonality relation of Eq. 5 we have the result

$$a_o = \pi^{1/4}$$
$$a_i = 0 \quad i \neq 0 \tag{25}$$

The relations of Eq. 25 together with the knowledge that the Laguerre network has been by-passed serve to characterize the given nonlinear system.

Now let us consider the inverse problem with respect to the same example. Suppose we are given the coefficients of Eq. 25 along with the associated information in the preceding paragraph. Our job is to synthesize the corresponding nonlinear system.

The guide for the synthesis is Eq. 18 which corresponds to Eq. 11 in the more complicated case. Following the general procedure for the synthesis described earlier it is readily seen that the resulting system is that shown in Fig. X-8. Figure X-8(a) shows how the synthesis takes form according to the formal dictates of Eq. 18. The simplified equivalent system obtained from Fig. X-8(a) by inspection is shown in Fig. X-8(b). We see that for the simple example considered the synthesized system consists solely of the "function generator," a component which in the more complicated case will form only a part of the synthesized system.

At this point it is of interest to note that we have at our disposal the two scale factors of the Laguerre and Hermite functions. For simplicity in the presentation of the basic concepts of Dr. Wiener's method, these scale factors have been chosen to be unity. In practice, they can be used to reduce the number of parameters, A_a, necessary to characterize the system. They are to be judiciously chosen on the basis of a priori knowledge of, or tests made on, the nonlinear system.

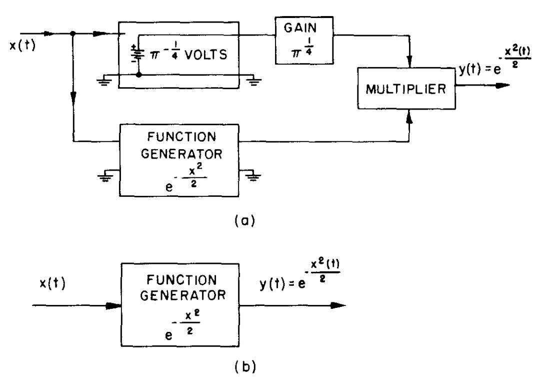

Fig. X-8

(a) Synthesis of the nonlinear characteristic $y = \exp -(x^2/2)$ according to the general procedure of Fig. X-7. (b) Equivalent reduced form of part (a).

In concluding this discussion of Dr. Wiener's method of nonlinear systems the question naturally arises as to the number of parameters, A_a, that may be necessary to characterize a practical system. In the simple example worked earlier, only one parameter was necessary. However, suppose we have a system which requires s Laguerre coefficients to sufficiently characterize that portion of the past of x(t) which influences the behavior of the system. Further suppose we decide that a sufficient approximation to the performance of the system is obtained by letting the indices $i, j, \ldots, h$ in Eq. 10 range from 0 to N - 1. Then there are N^s parameters (A_a) necessary to characterize the system. Without a doubt this number can become quite large in many practical cases. However, with the freedom that exists in nonlinear systems, one can hardly expect to apply such a general approach without considerable effort.

A. G. Bose

References

1. N. Wiener, Mathematical problems of communication theory, summer session lecture notes, M.I.T., 1953-1954, unpublished.
2. Y. W. Lee, J. Math. Phys. 11, 83-113 (1932).

C. PROPERTIES OF SECOND-ORDER AUTOCORRELATION FUNCTIONS

In the study of second-order autocorrelation functions the following two definitions are used:

$$\phi_{111}(\tau_1, \tau_2) = \overline{f_1(t)\, f_1(t+\tau_1)\, f_1(t+\tau_1+\tau_2)} \tag{1}$$

$$\phi^*_{111}(\tau_1, \tau_2) = \overline{f_1(t)\, f_1(t+\tau_1)\, f_1(t+\tau_2)} \tag{2}$$

where $f_1(t)$ is a stationary time series.

By shifting the time origin in Eq. 1 we obtain the following relations between the two definitions:

$$\left.\begin{aligned}
\phi_{111}(\tau_1, \tau_2) &= \phi^*_{111}(\tau_2, -\tau_1) && \text{(a)}\\
\phi_{111}(-\tau_1, \tau_2) &= \phi^*_{111}(\tau_1, \tau_2) && \text{(b)}\\
\phi_{111}(\tau_1, -\tau_2) &= \phi^*_{111}(-\tau_1, -\tau_2) && \text{(c)}\\
\phi_{111}(-\tau_1, -\tau_2) &= \phi^*_{111}(-\tau_2, \tau_1) && \text{(d)}
\end{aligned}\right\} \tag{3}$$

From the definition of $\phi^*_{111}(\tau_1, \tau_2)$ it is clear that

$$\phi^*_{111}(\tau_1, \tau_2) = \phi^*_{111}(\tau_2, \tau_1) \tag{4}$$

Making use of this relation, we obtain from 3(a) and 3(d) the relations

$$\phi_{111}(\tau_1, \tau_2) = \phi^*_{111}(-\tau_1, \tau_2) \tag{3a'}$$

$$\phi_{111}(-\tau_1, -\tau_2) = \phi^*_{111}(\tau_1, -\tau_2) \tag{3d'}$$

The relations between $\phi_{111}(\tau_1, \tau_2)$ and $\phi^*_{111}(\tau_1, \tau_2)$ as given by Eqs. 3b, c, a', and d' are illustrated in Fig. X-9. From these relations it can be shown that the $\phi_{111}(\tau_1, \tau_2)$ plane is the $\phi^*_{111}(\tau_1, \tau_2)$ plane rotated about the τ_2 axis by 180°. That is, the $\phi_{111}(\tau_1, \tau_2)$ plane is the mirror image of the $\phi^*_{111}(\tau_1, \tau_2)$ plane about the τ_2 axis. Consequently, given the properties of $\phi^*_{111}(\tau_1, \tau_2)$, we can easily establish the corresponding properties of $\phi_{111}(\tau_1, \tau_2)$ and vice versa.

By a process similar to that used to derive Eq. 3, we obtain from Eq. 1 the relation

$$\phi_{111}(\tau_1, \tau_2) = \phi_{111}(-\tau_2, -\tau_1) = \phi_{111}(-\tau_1, \tau_1+\tau_2) = \phi_{111}(\tau_2, -\tau_1-\tau_2) \tag{5}$$

This shows that a knowledge of one quadrant of $\phi_{111}(\tau_1, \tau_2)$ is sufficient to determine the

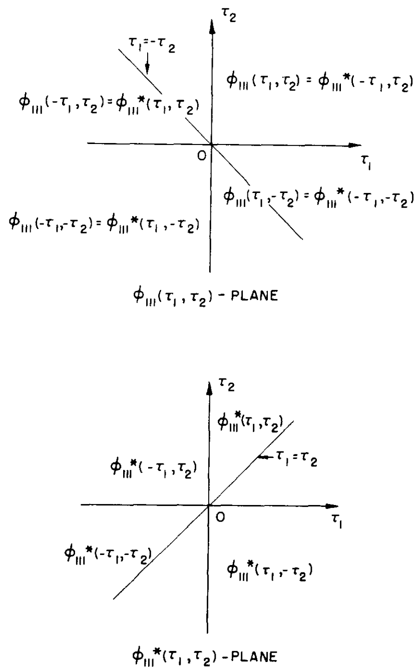

Fig. X-9

Relation between $\phi_{111}(\tau_1, \tau_2)$ and $\phi_{111}^*(\tau_1, \tau_2)$. The $\phi_{111}(\tau_1, \tau_2)$ plane is the $\phi_{111}^*(\tau_1, \tau_2)$ plane rotated 180° about the τ_2 axis.

remaining three quadrants, although such a procedure as indicated by this equation would not, in general, be the most practical method for constructing the remaining quadrants.

Now let us consider symmetry properties of second-order correlation functions. From Eq. 4 we see that $\phi_{111}^*(\tau_1, \tau_2)$ is always symmetrical about the line $\tau_1 = \tau_2$. It follows from this fact, and the mirror image relationship between the $\phi_{111}(\tau_1, \tau_2)$ and $\phi_{111}^*(\tau_1, \tau_2)$ planes, that $\phi_{111}(\tau_1, \tau_2)$ is always symmetrical about the line $\tau_1 = -\tau_2$.

It is of interest to show that if f(t) is a stationary time series such that the statistical behavior of f(t) is identical with the statistical behavior of the time series f(-t), then $\phi_{111}(\tau_1, \tau_2)$ is symmetrical about the line $\tau_1 = \tau_2$ in addition to being symmetrical about the line $\tau_1 = -\tau_2$. Symmetry about the line $\tau_1 = \tau_2$ means that $\phi_{111}(\tau_1, \tau_2) = \phi_{111}(\tau_2, \tau_1)$. Sufficient conditions for this equality can be established by expressing $\phi_{111}(\tau_1, \tau_2)$ as an ensemble average.

$$\phi_{111}(\tau_1, \tau_2) = \int_{-\infty}^{\infty} \int_{-\infty}^{\infty} \int_{-\infty}^{\infty} xyz \, P\left(x, y_{\tau_1}, z_{\tau_1+\tau_2}\right) dx \, dy \, dz \tag{6}$$

In this expression $P\left(x, y_{\tau_1}, z_{\tau_1+\tau_2}\right)$ is the third probability density of f(t). The subscripts of the variables denote the time of observation relative to the time $\tau = 0$ when the variable with no subscript (x in this particular expression) is observed. Using this notation we can write

$$\phi_{111}(\tau_2, \tau_1) = \int_{-\infty}^{\infty} \int_{-\infty}^{\infty} \int_{-\infty}^{\infty} x'y'z' \, P\left(x', y'_{\tau_2}, z'_{\tau_1+\tau_2}\right) dx' \, dy' \, dz' \tag{7}$$

Now, in Eq. 7 let us change the dummy variables of integration. Let $x' = z$, $y' = y$, and z' = x. Then Eq. 7 becomes:

$$\phi_{111}(\tau_2, \tau_1) = \int_{-\infty}^{\infty} \int_{-\infty}^{\infty} \int_{-\infty}^{\infty} xyz\ P\left(x_{\tau_1+\tau_2}, y_{\tau_2}, z\right) dx\ dy\ dz \tag{8}$$

To put this equation into a form convenient for comparison to Eq. 6, let us translate the τ axis to establish the reference axis (τ=0) at the time when the variable x is observed. The result is:

$$\phi_{111}(\tau_2, \tau_1) = \int_{-\infty}^{\infty} \int_{-\infty}^{\infty} \int_{-\infty}^{\infty} xyz\ P\left(x, y_{-\tau_1}, z_{-\tau_1-\tau_2}\right) dx\ dy\ dz \tag{9}$$

Comparing Eqs. 6 and 9 we see that a sufficient condition for the existence of symmetry about the line $\tau_1 = \tau_2$ is

$$P\left(x, y_{\tau_1}, z_{\tau_1+\tau_2}\right) = P\left(x, y_{-\tau_1}, z_{-\tau_1-\tau_2}\right) \tag{10}$$

This relation clearly holds for all stationary time series f(t) which have the same statistical behavior as the corresponding time series f(-t). If f(t) is a periodic function, Eq. 10 will hold, and thus there will be symmetry about the line $\tau_1 = \tau_2$ for all functions having a time origin about which the function is symmetrical.

It has been shown that $\phi_{111}(\tau_1, \tau_2)$ is always symmetrical about the line $\tau_1 = -\tau_2$ and is sometimes symmetrical about the line $\tau_1 = \tau_2$. The question naturally arises as to the existence of symmetry about the τ_1 and τ_2 axes. It is next shown that, with the exception of functions which give a constant second-order autocorrelation function, symmetry about the τ_1 and τ_2 axes is not present. This result will be proved by the method of contradiction.

By performing a translation of the time origin in Eqs. 1 and 2, it can be shown that if symmetry exists about either the τ_1 or τ_2 axis, then it exists about both axes. Hence, for the proof it is sufficient to show that the assumption of symmetry about the τ_2 axis leads to a contradiction.

The assumption is

$$\phi_{111}(\tau_1, \tau_2) = \phi_{111}(-\tau_1, \tau_2) \tag{11}$$

Using this relation and Eq. 3a' we obtain the relation

$$\phi_{111}(-\tau_1, \tau_2) = \phi^{*}_{111}(-\tau_1, \tau_2) \tag{12}$$

Expressing $\phi_{111}(-\tau_1, \tau_2)$ in terms of definition 2,

$$\phi_{111}(-\tau_1, \tau_2) = \phi^*_{111}(-\tau_1, \tau_2 - \tau_1) \tag{13}$$

Hence, from Eqs. 12 and 13

$$\phi^*_{111}(-\tau_1, \tau_2) = \phi^*_{111}(-\tau_1, \tau_2 - \tau_1) \tag{14}$$

If τ_1 is held fixed in Eq. 14, $\phi^*_{111}(-\tau_1, \tau_2)$ is periodic with respect to τ_2 with a period equal to the value of τ_1. This result is a contradiction when $f_1(t)$ is a random stationary time series, for the second-order autocorrelation function of a random function is not periodic with respect to either τ_2 or τ_1. The result is also a contradiction when $f_1(t)$ is a periodic function, for the second-order autocorrelation of a periodic function is periodic with respect to τ_2 for a given τ_1 but the period is independent of τ_1. Hence assumption 11 leads to a contradiction. This proves that $\phi_{111}(\tau_1, \tau_2)$ is not symmetrical with respect to the τ_1 or τ_2 axes except for the degenerate case in which $\phi_{111}(\tau_1, \tau_2)$ is a constant.

Y. W. Lee, A. G. Bose, J. Y. Hayase

D. FIELD MAPPING BY CROSSCORRELATION

The problem of determining the location of n sources of independent random stationary time series by the method of crosscorrelation has been considered under restricted conditions.

The sources lying on a plane are designated by S_j, where $j = 1, \ldots, n$, as shown in Fig. X-10. On the same plane, three points, L_i, $i = 1, 2, 3$, forming an equilateral triangle, are chosen as listening posts. The separation between these points is d. The signals received at L_i are

$$g_i(t) = \sum_{j=1}^{n} f_j(t - k\,d_{ij}) \tag{1}$$

where $f_j(t) \geqslant 0$ is the signal generated by S_j, d_{ij} is the distance between the points S_j and L_i, and k is the reciprocal of the velocity of light. The second-order crosscorrelation function of $g_i(t)$ is*

---

*The definition of the crosscorrelation function is similar to the definition of the autocorrelation function, $\phi^*_{111}(\tau_1, \tau_2)$, discussed in subsection C.

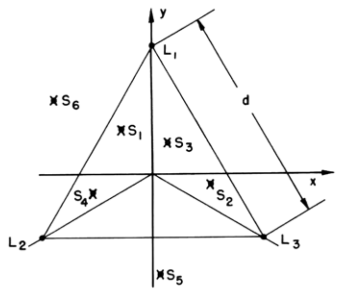

Fig. X-10

Distribution of sources and the location of listening posts.

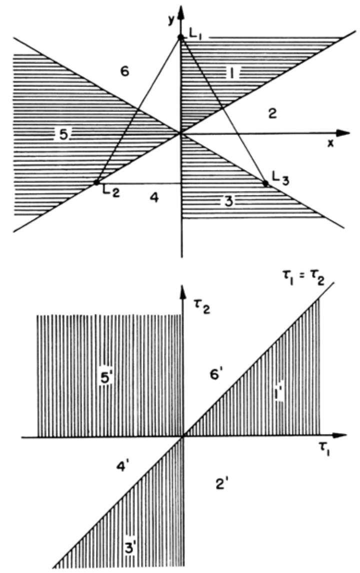

Fig. X-11

Relation between the areas in which sources S_i lie and the areas in which points $\left(\tau_1^{(i)}, \tau_2^{(i)}\right)$ lie.

$$\phi^*_{123}(\tau_1, \tau_2) = \overline{g_1(t)\, g_2(t+\tau_1)\, g_3(t+\tau_2)}$$

$$= \sum_{j=1}^{n} \sum_{\ell=1}^{n} \sum_{p=1}^{n} \overline{f_j(t - kd_{1j})\, f_\ell(t + \tau_1 - kd_{2\ell})\, f_p(t + \tau_2 - kd_{3p})} \qquad (2)$$

As a consequence of the independence of the sources, Eq. 2 is equivalent to

$$\phi^*_{123}(\tau_1, \tau_2) = \sum_{j=1}^{n} \overline{f_j(t - kd_{1j})\, f_j(t+\tau_1 - kd_{2j})\, f_j(t+\tau_2 - kd_{3j})}$$

$$+ \sum_{j=1}^{n} \sum_{\substack{\ell=1 \\ \ell \neq p}}^{3} \sum_{p=1}^{3} a_{j\ell p}\, \overline{f_j(t+\tau_{\ell-1} - kd_{\ell j})\, f_j(t+\tau_{p-1} - kd_{pj})}$$

$$+ \text{constant terms} \quad (n > 1) \qquad (2a)$$

where $\tau_0 = 0$. The value of $\phi^*_{123}(\tau_1, \tau_2)$ at

$$\left.\begin{aligned} \tau_1^{(i)} &= k(d_{2i} - d_{1i}) \\ \tau_2^{(i)} &= k(d_{3i} - d_{1i}) \end{aligned}\right\} \qquad (3)$$

is

$$\phi^{*}_{123}\left(\tau_1^{(i)}, \tau_2^{(i)}\right) = \overline{f_i^3\,(t - k\,d_{1i})} + A\,\overline{f_i^2(t - k\,d_{1i})}$$

$$+ \sum_{\substack{j=1\\ j\neq i}}^{n} \overline{\left\{f_j(t - k\,d_{ij})\, f_j\left(t + \tau_1^{(i)} - k\,d_{2j}\right) f_j\left(t + \tau_2^{(i)} - k\,d_{3j}\right)\right\}}$$

$$+ \sum_{\substack{j=1\\ j\neq i}}^{n} \sum_{\substack{\ell=1\\ \ell\neq p}}^{3} \sum_{p=1}^{3} a_{j\ell p}\, \overline{f_j\left(t + \tau^{(i)}_{\ell-1} - k\,d_{\ell j}\right) f_j\left(t + \tau^{(i)}_{p-1} - k\,d_{pj}\right)}$$

$$+ \text{other constant terms} \quad (n > 1) \tag{4}$$

In the simple case where $n = 1$,

$$\phi^{*}_{123}\left\{k(d_{21} - d_{11}),\quad k(d_{31} - d_{11})\right\} = \overline{f_1^3(t - k\,d_{11})} \tag{5}$$

Since it can be shown that

$$\overline{f_j^3(t)} \geq \overline{f_j(t)\, f_j(t + \tau_1)\, f_j(t + \tau_2)} \tag{6}$$

the time displacements $\tau_1^{(1)}$ and $\tau_2^{(1)}$, which are related to the distances d_{11}, d_{21}, and d_{31} by

$$\tau_1^{(1)} = k(d_{21} - d_{11}), \quad \tau_2^{(1)} = k(d_{31} - d_{11}) \tag{7}$$

can be determined by plotting $\phi^{*}_{123}(\tau_1, \tau_2)$ vs. τ_1, τ_2 with the aid of a correlator.

When $n > 1$, the summation terms in Eq. 4 may introduce an error in the measured $\tau_1^{(i)}$ and $\tau_2^{(i)}$. It can be shown that this error depends on the relative position of the points S_j, and the nature of the random function $f_j(t)$. If the summation terms introduce negligible error on the measured $\tau_1^{(i)}$ and $\tau_2^{(i)}$, then those determine the location of S_i.

The difference in the distances $d_{2i} - d_{1i}$, $d_{3i} - d_{1i}$, and $d_{2i} - d_{3i}$ can be expressed in terms of $\tau_1^{(i)}$ and $\tau_2^{(i)}$ by the equations

$$\left.\begin{aligned} d_{2i} - d_{1i} &= \frac{\tau_1^{(i)}}{k} \\ d_{3i} - d_{1i} &= \frac{\tau_2^{(i)}}{k} \\ d_{2i} - d_{3i} &= \frac{\tau_1^{(i)} - \tau_2^{(i)}}{k} \end{aligned}\right\} \tag{8}$$

Three families of hyperbolas, whose respective foci are L_1 and L_2, L_1 and L_3, and L_2 and L_3, are available for determining the location of S_i. Any two families of hyperbolas are sufficient to determine the location of S_i which is given by the intersection of a branch from each family. The choice of the two families is dictated by the geometrical configuration of S_i and the fixed points, L_1, L_2, and L_3. The differences in the distances from the two foci to S_i for a given family are given by Eq. 8. This hyperbolic grid system is the same as that of Loran.

With the restriction that

$$\left.\begin{array}{l} |\tau_1^{(i)}| \leqslant k\,d \\ \text{and} \\ |\tau_2^{(i)}| \leqslant k\,d \end{array}\right\} \tag{9}$$

the relation between the areas in which the sources, S_i, and the points, $\left(\tau_1^{(i)}, \tau_2^{(i)}\right)$, lie can be shown as in Fig. X-11. The correspondence between the areas in the xy plane and the $\tau_1\tau_2$ plane is shown by primed integers and unprimed integers.

J. Y. Hayase

E. CORRELATION DETECTION OF A PERIODIC SIGNAL MULTIPLIED BY NOISE

If a periodic signal S'(t) is multiplied by statistically stationary random noise, the product may be written

$$S'(t)\ N'(t) = \left[S(t) + \bar{S}\right]\left[N(t) + \bar{N}\right] \tag{1}$$

where S and N are the mean values of S'(t) and N'(t), respectively. If $\bar{N}$ is not zero, the periodic signal can be detected by autocorrelation, but if it is zero, detection by autocorrelation alone is not possible.

By filtering in the frequency domain, Eq. 1 may be reduced to S(t) N(t). For this case, the autocorrelation function of the product is the product of the autocorrelation functions

$$\phi_{SN}(\tau) = \phi_S(\tau)\ \phi_N(\tau) \tag{2}$$

Although $\phi_S(\tau)$ is periodic, $\phi_N(\tau)$ tends to zero for τ large, so that, in general, the periodic signal may not be detected by autocorrelation. If the factors of Eq. 2 are separated, or, if $\phi_N(\tau)$ is made to approach a constant other than zero, detection by autocorrelation is possible.

The factors may be separated by taking the logarithm, thus

$$\log|SN| = \log|S| + \log|N| \tag{3}$$

$$\phi(\tau) = \phi_{\log S}(\tau) + \phi_{\log N}(\tau) + 2\, \overline{\log N(t)}\; \overline{\log S(t)} \tag{4}$$

The periodic signal is revealed by the first term of Eq. 4; the other terms approach constants for τ large.

The noise factor of Eq. 2 may be made nonzero for τ large by a nonlinear operation on the product S(t) N(t). If the product S(t) N(t) is applied as an input to a nonlinear device the transfer characteristic of which may be written

$$f(x) = \sum_{0}^{\infty} A_n x^n \tag{5}$$

then the output autocorrelation function may be written

$$\begin{aligned}\phi(\tau) &= \overline{\sum_{n=0}^{\infty} A_n \left[S(t)\, N(t)\right]^n \sum_{j=0}^{\infty} A_j \left[S(t+\tau)\, N(t+\tau)\right]^j} \\ &= \sum_{n=0}^{\infty} A_n^2\, \overline{\left[S(t)\, S(t+\tau)\right]^n}\; \overline{\left[N(t)\, N(t+\tau)\right]^n} \\ &\quad + \sum_{\substack{n=0 \\ n\neq j}}^{\infty} \sum_{j=0}^{\infty} A_n A_j\, \overline{S(t)^n\, S(t+\tau)^j}\; \overline{N(t)^n\, N(t+\tau)^j}\end{aligned} \tag{6}$$

Some noise terms having nonzero means are multiplied by signal terms. Since it is not possible for a random function raised to an even power to have a zero mean, any nonlinear device having even-power terms in the power series expansion of its transfer characteristic permits the detection of the periodic signal. If the probability density function of N(t) has even symmetry about the origin, then the odd-power terms of Eq. 5 do not aid in the detection of the periodic signal; but if not, the odd-power terms may aid.

A commercially available logarithmic device and a full-wave linear rectifier provided the more interesting transfer characteristics for the experimental work. The characteristics are

$$\text{Limiter (odd)} \qquad y = \begin{cases} k_1 \log k_2 x & a \leqslant x \leqslant b \\ k_3 x & -a \leqslant x \leqslant a \\ -k_1 \log(-k_2 x) & -b < x \leqslant -a \end{cases} \tag{7}$$

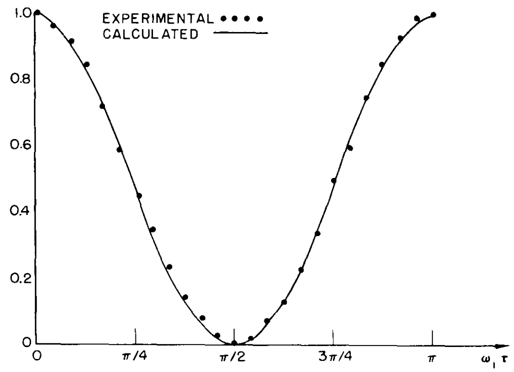

Fig. X-12

$\phi(\tau)$ for full-wave S.

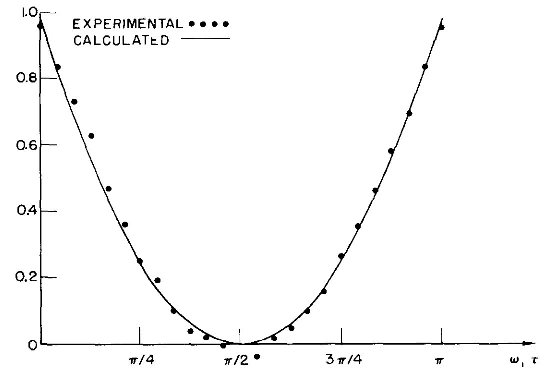

Fig. X-13

$\phi(\tau)$ for full-wave log S.

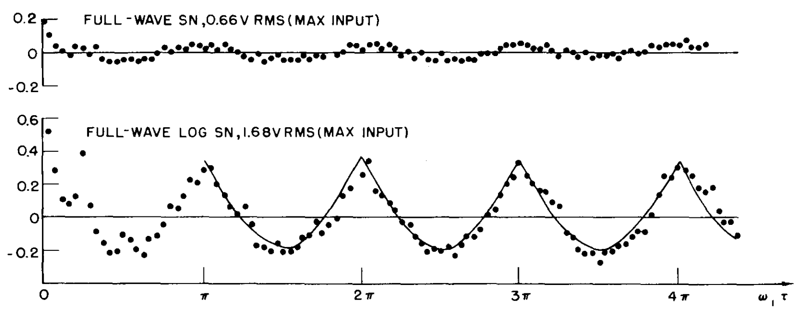

Fig. X-14

$\phi(\tau)$ for full-wave log SN and full-wave SN.

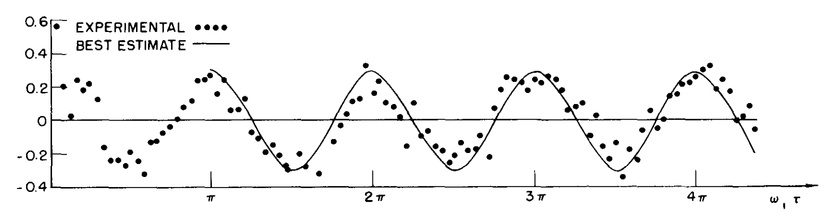

Fig. X-15

$\phi(\tau)$ for full-wave SN.

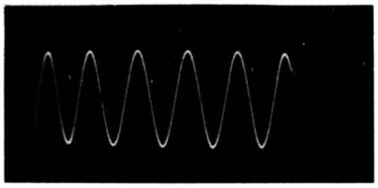

a. S, sine wave.

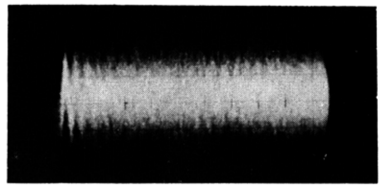

b. N, band-limited noise.

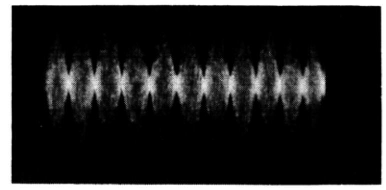

c. SN, sine wave times noise

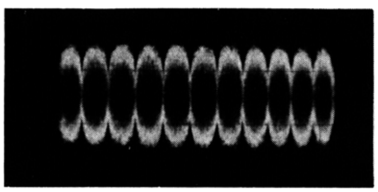

d. Limiter-log SN.

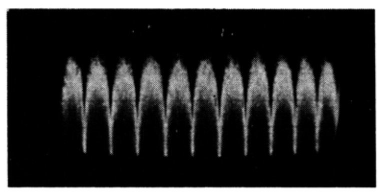

e. Full-wave log SN.

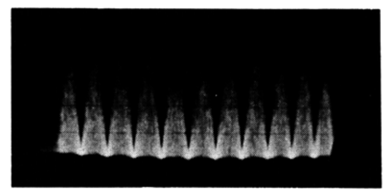

f. Full-wave SN.

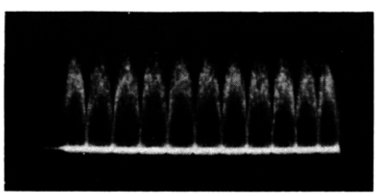

g. Half-wave log SN.

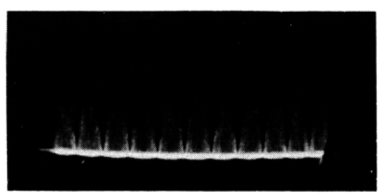

h. Half-wave SN.

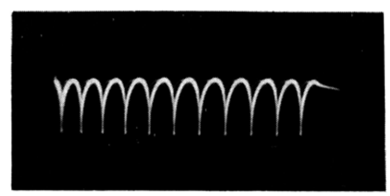

i. Full-wave log S.

Fig. X-16

Oscilloscope photographs: time scale, 1 msec; sine wave, 5.1 kc/sec; noise, 4 kc/sec centered at 21.9 kc/sec.

Full-wave (even) $$y = \begin{cases} k_4 \log |k_2 x| & a \leqslant |x| < b \\ |k_5 x| & 0 < |x| \leqslant a \end{cases} \tag{8}$$

Full-wave (even) $$y = |k_6 x| \tag{9}$$

If the input of an ideal logarithmic device is $E \sin \omega_1 t$, then the output is $y = B \log_\epsilon |E \sin \omega_1 t|$, and the autocorrelation function of the output is

$$\phi(\tau) = (B \log_\epsilon E)^2 + \frac{B^2 \pi^2}{2} \left[\left(\frac{\omega_1 \tau}{\pi} \right)^2 - \left(\frac{\omega_1 \tau}{\pi} \right) + \frac{1}{6} \right] \tag{10}$$

where B is determined by the characteristics of the log device and the gain of the output amplifiers. The autocorrelation function for the output of a full-wave linear rectifier, $y = |E \sin \omega_1 t|$ is

$$\phi(\tau) = \frac{E^2}{\pi} \left[\left(\frac{\pi}{2} - \omega_1 \tau \right) \cos \omega_1 \tau + \sin \omega_1 \tau \right] \tag{11}$$

Calculated and experimental results are shown in Figs. X-12 and X-13 for these two cases.

Figure X-14 shows the experimentally obtained autocorrelation function for full-wave log SN and full-wave SN for identical correlator control settings. S is a sine wave and N is band-limited gaussian noise. Figure X-15 shows the autocorrelation function for full-wave SN for increased correlator sensitivity (and increased error). The similarity of the curves in Fig. X-12 and X-14 suggests that the factors did separate as indicated by Eq. 3. The autocorrelation function for limiter-log SN does not reveal the periodic component.

Oscilloscope photographs such as those in Fig. X-16 proved to be a valuable aid.

C. E. McGinnis

F. AN IMPROVEMENT IN THE DIGITAL ELECTRONIC CORRELATOR

The correlator employs a compensating circuit to minimize drift error. When processing low-frequency information (dc to 500 cps), this compensating circuit acts upon a reference voltage of zero volts which is applied to the inputs of the correlator in intervals alternate to those during which the signals to be correlated are applied. The intervals are such that samples taken by the machine are alternately signal and reference samples. Difficulty in establishing a constant reference voltage of zero volts during the reference sample intervals has led to the development of a very satisfactory circuit for this purpose.

The circuit previously in use consisted of two tubes in series working between +150 volts and -150 volts. These tubes were alternately gated on and off, and their junction was connected to the input tube of the correlator. A potentiometer in series with the two tubes adjusted the voltage at the junction, during the on time, to zero. During the off time, the grid of the correlator input tube was at high impedance and free to receive the signal fed to it through a series resistor. This method suffered from the obvious difficulty of being very dependent upon the tube characteristics and upon the stability of the plus and minus B supplies.

The improved circuit is shown in Fig. X-17. During the intervals for which both sections of the tube are on, there is a very small resistance (about 150 ohms) between points a and b and the signal, f(t), passes freely to the grid of the correlator input tube. During the intervals for which both sections of the 6AS7 are off, the grid of the correlator tube is isolated from the source f(t), and it returns to zero. This circuit has the advantage of being almost completely independent of changes in the 6AS7 characteristics.

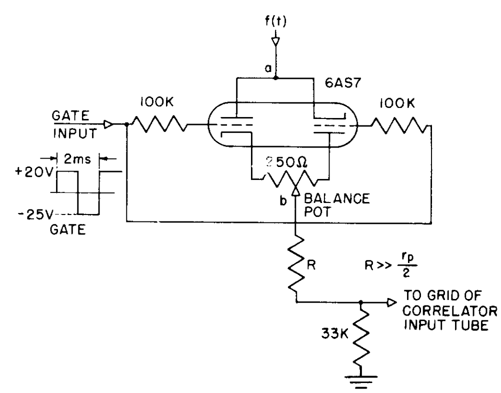

Fig. X-17

Improved circuit for the digital correlator. The time function f(t) is the function to be correlated (10 volts maximum either side of zero). It is to be obtained from a low impedance dc coupled source.

Since there is no B voltage applied to the 6AS7, and since the filament voltage is reduced to minimize hum, the tube life is long. This circuit, in conjunction with the compensator, enables the machine to process low-frequency information with an accuracy of the same order of magnitude as that obtained when the machine is ac coupled and processing higher frequency information.

A. G. Bose

G. MEASUREMENT OF INDUSTRIAL PROCESS BEHAVIOR

Experimental determinations of the transfer function $H(\omega)$ or impulse response $h(t)$ of industrial processes are complicated by the presence of noise and by the difficulty of applying suitable sinusoidal or impulsive driving functions to massive industrial systems. The statistical method of determining system characteristics overcomes these difficulties (1). This method uses as the driving function the random fluctuations already existing in the input variable. The result is not usually affected by random fluctuations originating within the process.

A heat transfer process frequently encountered in industry has been chosen for experimental study. In this process, a liquid flowing through a copper tube is heated by water flowing through a concentric copper shell. Thermocouples are used to measure the temperatures of the liquids. When cold water from the building mains flows through the tube and a mixture of hot and cold water from the same mains flows through the shell, the shell and tube temperatures fluctuate as shown in Fig. X-18.

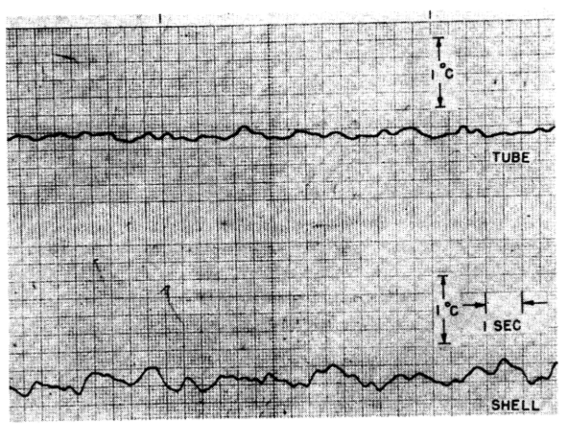

Fig. X-18
Temperature fluctuations in shell and tube of heat exchanger.

Preliminary results obtained with the low-frequency multisignal correlator (2), while encouraging, indicate that practical application of the method must await further refinement of the measuring system.

S. G. Margolis

References

1. Y. W. Lee, Technical Report No. 181, Research Laboratory of Electronics, M.I.T., Sept. 1, 1950.

2. D. G. C. Hare, Final engineering report, Design and construction of low frequency multi-signal correlator for the Air Force Cambridge Research Center, Contract No. AF19(122)-213.